Highlights:

Dietary alkylresorcinols prevent muscle atrophy.

Alkylresorcinols improve a disturbed energy metabolism caused by muscle atrophy.

Alkylresorcinols modify the disruption to fatty acid metabolism induced by lipid autophagy.

Dietary supplementation with alkylresorcinols prevents muscle atrophy through a shift of energy supply

Shigeru Hiramoto[a], Nobuhiro Yahata[a], Kanae Saitoh[b], Tomohiro Yoshimura[b], Yao Wang[b], Shigeto Taniyama[b], Takeshi Nikawa[c], Katsuyasu Tachibana[b], Katsuya Hirasaka[b, d, *]

[a]Healthcare Research Center, Nisshin Pharma Inc., Saitama, Japan 3568511

[b]Graduate School of Fisheries and Environmental Sciences, [d]Organization for Marine Science and Technology, Nagasaki University, Nagasaki, Japan 8528521

[c]Department of Nutritional Physiology, Institute of Medical Nutrition, Tokushima University Medical School, Tokushima, Japan 7708503

Running head: Effect of oral alkylresorcinols on muscle atrophy

***Corresponding author:** Katsuya Hirasaka, Ph. D.

Organization for Marine Science and Technology, Nagasaki University

1-14 Bunkyo-machi, Nagasaki, 8528521 JAPAN

Email: hirasaka@nagasaki-u.ac.jp

Phone: +81-(95) 819-2858, Fax: +81-(95) 819-2858

Abstract

It has been reported that phytoextracts, that contain alkylresorcinols (ARs) protect against severe myofibrillar degeneration found in isoproterenol-induced myocardial infarction. In this study, we examined the effect of dietary ARs derived from wheat bran extracts on muscle atrophy in denervated mice. The mice were divided into the following four groups: 1) sham-operated (control) mice fed with normal diet (S-ND); 2) denervated mice fed with normal diet (D-ND); 3) control mice fed with ARs-supplemented diet (S-AR); and, 4) denervated mice fed with ARs-supplemented diet (D-AR). The intake of ARs prevented the denervation-induced reduction of the weight of the hind limb muscles and the myofiber size. However, the expression of ubiquitin ligases and autophagy-related genes, which is associated with muscle proteolysis, was slightly higher in D-AR than in D-ND. Moreover, the abundance of the autophagy marker p62 was significantly higher in D-AR than in D-ND. Muscle atrophy has been known to be associated with a disturbed energy metabolism. The expression of pyruvate dehydrogenase kinase 4 (PDK4), which is related to fatty acid metabolism, was decreased in D-ND as compared with that in S-ND. In contrast, dietary supplementation with ARs inhibited the decrease of PDK4 expression caused by denervation. Furthermore, the abnormal expression pattern of genes related to the abundance of lipid droplets-coated proteins that was induced by denervation, was improved by ARs. These results raise the

possibility that dietary supplementation with ARs modifies the disruption of fatty acid metabolism induced by lipid autophagy, resulting in the prevention of muscle atrophy.

Key words: alkylresorcinols; muscle atrophy; fatty acid metabolism; lipid autophagy

1. Introduction

A decline in muscle mass termed muscle atrophy, has been observed under the conditions of disuse (e.g., immobilization, denervation, muscle unloading), fasting, aging, and several disease states including cancer cachexia, sepsis, diabetes mellitus, and chronic renal failure [1, 2]. Muscle atrophy can be caused by decreased protein synthesis and/or increased proteolysis. We previously reported that an accumulation of ubiquitinated proteins was observed in the quadriceps femoris muscle of bedridden volunteers and the gastrocnemius (GA) muscle of spaceflight-exposed rats, indicating that the ubiquitin proteasome system plays an important role in the degradation of proteins in atrophied muscle [3, 4]. It is true that mice deficient in the muscle-specific ubiquitin ligases MuRF-1 and atrogin-1/MAFbx showed resistance against denervation-induced muscle loss [5, 6]. The expression of ubiquitin ligases and autophagy-related genes such as LC3 and Gabarap in muscle was reported to be induced by denervation or fasting [7]. Furthermore, it has been reported that denervation-induced protein loss in muscles involved proteolysis rather decreased protein synthesis [8, 9]. Thus, the inhibition of proteolysis is important in the prevention of muscle loss in some atrophy models.

Under the condition of disuse, muscle atrophy causes a switch in muscle fiber type. Previous studies have demonstrated that denervation induces the transformation of slow oxidative fibers to fast glycolytic fibers in rat soleus muscle [10, 11]. In addition, we have

previously reported that mitochondrial dislocation and dysfunction were found in disused muscle [12]. Furthermore, the results of gene ontology data showed that the expression of genes associated with “fatty acid catabolic process” had significantly decreased after denervation [13]. Thus, it appears that muscle atrophy induces a metabolic shift from oxidative to glycolytic metabolism.

Phenolic compounds derived from plants have several benefits to human health and reduce the risks of developing cardiovascular disease and cancer [14]. Whole grains contain various phenolic compounds and an increased intake of whole grains in patients with obesity, type II diabetes, and cardiovascular disease has been shown to lower blood pressure, increase insulin sensitivity, and improve glucose and lipid metabolism [15, 16, 17]. One of the major groups of phenolic compounds in whole-grain cereals is the 5-n-alkylresorcinols (ARs), which comprise approximately 0.015–0.3% of the dry weight of wheat and rye grains [18]. It has been reported that the intake of ARs suppressed obesity and glucose intolerance induced by a high-fat, high-sucrose diet, by increasing insulin sensitivity and cholesterol excretion in mice [19]. Meanwhile, phenolic compounds obtained from olive oil are known to have a protective effect against muscle atrophy and also improve high fat diet-induced insulin resistance in skeletal muscle [20, 21]. In the present study, we examined the effect of ARs, phenolic compounds derived from wheat bran extracts, on denervation-induced muscle atrophy.

2. Materials and Methods

2.1 Isolation of ARs

ARs were isolated from wheat bran M (Nisshin seifun, Tokyo, Japan) as described in a previous report [19].

2.2 Animal model (denervation)

Male C57BL/6N mice (Kyudo, Kumamoto, Japan) aged 6 weeks were housed in a room maintained at 24 ± 1 °C on a 12-h light/dark cycle with food (Oriental Yeast Company, Tokyo, Japan) and water available ad libitum. The mice were divided into four groups: 1) sham-operated (control) mice fed with normal diet (S-ND, n=5); 2) denervated mice fed with normal diet (D-ND, n=6); 3) control mice fed with ARs diet (S-AR, n=5); and, 4) denervated mice fed the ARs diet (D-AR, n=6). Briefly, after acclimatization for 1 week, an ARs-supplemented diet (0.4%, w/w) or normal diet was given to the mice for 4 weeks. After then, the sciatic nerve of the right leg was cut and a 5-mm piece was excised under anesthesia. During the development of disuse-induced muscle atrophy, the mice continued to receive the normal or ARs-supplemented diet until the termination of the experiment 6 days later. The α-starch content of the ARs-supplemented diet was reduced to adjust for the composition of other nutrients and comprised the normal diet (based on AIN-93M) mixed with purified ARs

98 (0.4% w/w). The hind limb skeletal muscles [the tibialis anterior (TA), extensor digitorum
99 longus (EDL), GA, and soleus (SO)] were isolated at the time of sacrifice. After measuring
100 their wet weight, the skeletal muscles were immediately frozen in chilled isopentane and
101 liquid nitrogen and were stored at −80 °C until analysis. All animal experiments involving
102 denervation were approved by the Committee on Animal Experiments of Nagasaki
103 University, and were performed according to the guidelines for the care and use of laboratory
104 animals prescribed by the University.
105
106 *2.3 Quantitative reverse transcription (RT)-polymerase chain reaction (PCR)*
107 Total RNA was extracted from mouse GA muscle using an acid guanidinium
108 thiocyanate-phenol-chloroform mixture (ISOGEN™; Nippon Gene, Tokyo, Japan).
109 Quantitative RT-PCR was performed with the appropriate primers and SYBR® Green dye
110 using a real-time PCR system (ABI Real-Time PCR Detection System; Applied Biosystems,
111 Foster City, CA, USA), as described previously [22]. The oligonucleotide primers used for
112 PCR are shown in Supplemental Table 1. We used 18S ribosomal RNA as an internal
113 standard gene.
114
115 *2.4 Immunoblotting*

116 The mouse GA muscle was prepared in 50 mM Tris-HCl buffer, pH 7.5, containing
117 150 mM NaCl, 1% Triton™ X-100, and a protease inhibitor cocktail containing
118 ethylenediaminetetraacetic acid (Roche Diagnostics, Tokyo, Japan), and the samples were
119 homogenized using a sonicator. The Pierce BCA assay (Pierce, Rockford, IL, USA) was used
120 to quantify proteins. Protein samples were combined with 4× sample buffer (250 mM Tris-
121 HCl, 8% sodium dodecyl sulfate, 40% glycerol, 8% β-mercaptoethanol, and 0.02%
122 bromophenol blue) and separated on a polyacrylamide gel. The proteins were transferred to a
123 polyvinylidene difluoride membrane and then probed with the appropriate primary antibody
124 according to the manufacturer's instructions. The primary antibodies used in this study were
125 anti-LC3b, anti-p62 (Sigma Aldrich, St. Louis, MO, USA), and anti-GAPDH (Santa Cruz
126 Biotechnology, Dallas, TX, USA). The secondary antibody used was donkey anti-rabbit IgG
127 at 1:5000 dilution (GE Healthcare, Little Chalfont, UK). Membranes were developed using
128 Amersham™ ECL™ western blotting detection reagents (GE Healthcare).
129
130 *2.5 Hematoxylin and eosin staining and measurement of cross-sectional area*
131 The isolated GA muscle of mice was immediately frozen in chilled isopentane and
132 liquid nitrogen and stored at −80 °C until analysis. Sections of the GA muscle (5 μm
133 thickness) were fixed in ice-cold acetone. After fixation, the sections were stained with
134 hematoxylin and eosin. Images were acquired with a BIOREVO BZ-X710 fluorescence

135 microscope (Keyence, Osaka, Japan) using a camera and processed using BZ-II analysis
136 software (Keyence). At least 1000 cross-sectional areas (CSAs) of myofibers were measured
137 per sample. The data were expressed as the fiber size distribution.

138 *2.6 Statistical analysis*

139 All data were analyzed using one-way analysis of variance (ANOVA) using the
140 Excel-Toukei version 6.0 software (Statistics Survey System-development, Tokyo, Japan),
141 followed by Tukey-Kramer (for unequal number) test to identify which treatments were
142 significantly different. All data are expressed as mean ± SEM (n = 5–6). The p values < 0.05
143 were considered significantly different.

144

145 **Results**

146 *3.1 Effect of dietary ARs on muscle mass and myofiber size distribution in*
147 *denervation-induced muscle atrophy.*

148 It has been reported that extracts of *Labisia pumila var. alata*, which contain ARs,
149 gallic acid, and flavonoids, protect against isoproterenol-induced myocardial infarction
150 through the activation of anti-oxidant enzymes in rats [23]. To examine the potential
151 inhibitory effect of ARs on skeletal muscle atrophy, we compared the wet weights of several
152 muscles between sham-operated and denervated mice fed the normal or ARs-supplemented
153 diet. Consistent with previous report [19], there was no significant difference in the food

intake of the normal and ARs-supplemented diet groups (Table 1). Meanwhile, the body weights and fasting blood glucose levels of non-denervated mice fed the AR diet were lower than that of non-denervated mice fed the normal diet (fasting blood glucose: normal diet group = 3.68 ± 0.13 mmol/l; ARs-supplemented diet group =3.34 ± 0.14 mmol/l). The percentage of white adipose tissue to body weight was 3.06 ± 0.17% in the normal diet group and 2.23 ± 0.21% in the ARs-supplemented diet group. As shown in Fig. 1, the wet weights of skeletal muscles such as TA, EDL, GA, and SO normalized to body weight in D-ND decreased by 78, 85, 73, and 84% compared to those in sham-operated mice, respectively (Fig. 1). In contrast, the wet weights of TA, EDL, GA, and SO in the D-AR were 96, 115, 90, and 92% higher compared to the sham-operated mice, respectively (Fig. 1). The weights of the TA, EDL, and GA in the D-AR were higher than those in the D-ND.

The CSA of myofibers stained with hematoxylin and eosin in the S-ND was similar to that observed in the S-AR (Fig. 2). Denervation induced a decrease in the average CSA of myofibers. The size distributions of myofibers in D-ND and D-AR indicated a decrease in the proportion of fibers in CSA of 1000–2000 μm^2, and an increase in the proportion of those in CSA of <1000 μm^2, as compared with those in S-ND and S-AR (Fig. 2). In S-AR, as compared with S-ND, there was an increase in the proportion of myofibers in CSA of >1000 μm^2 and a decrease in the proportion of those in CSA of <1000 μm^2 (Fig. 2). Thus, the denervated mice that were fed the AR diet appeared to be resistant to muscle fiber atrophy.

3.2 Effect of dietary ARs on the proteolysis in muscle of denervated mice.

Muscle atrophy-associated ubiquitin ligases, such as MAFbx/Atrogin-1 and MuRF1, and autophagy contribute to skeletal muscle atrophy [5, 6]. It has been known that denervation is associated with an increase in the expression of the ubiquitin ligases MAFbx/Atrogin-1 and MuRF1 and the autophagy-related genes LC3b, Bnip3, Bnip3l, Beclin, and Gabarapl1 [24]. To investigate whether ARs suppress muscle atrophy through the activation of proteolysis, we examined the mRNA expression of the ubiquitin ligases and autophagy-related genes in the skeletal muscle of S-ND, D-ND, S-AR, and D-AR. The mRNA transcription of the ubiquitin ligases MAFbx/Atrogin-1 and MuRF1 in the skeletal muscle of denervated mice was significantly higher than that in the sham-operated mice (Fig. 3). The analysis of the expression of autophagy-related genes revealed that the expression of Gabarapl1 and p62 mRNA showed the same pattern as the expression of the ubiquitin ligases (Fig. 3).

Next, we investigated the effect of ARs on the activation of autophagy in muscle atrophy. The abundance of the active form of LC3 (LC3-II) in the skeletal muscle of denervated mice increased significantly, as compared with that in the sham-operated mice, whereas there was no difference between D-ND and D-AR in the abundance of LC3-II (Fig.

191 4). Interestingly, the abundance of the autophagy marker p62 was significantly higher in D-
192 AR than in D-ND (Fig. 4).
193
194 *3.3 Effect of dietary ARs on the expression of energy metabolism-related genes in*
195 *denervated mice.*
196 It has been known that the activation of autophagy contributes to energy balance by
197 degrading lipids as well as proteins [25]. To determine whether ARs affect energy
198 metabolism during muscle atrophy, we examined the mRNA expression of several energy
199 metabolism-related genes in atrophied muscle. There was a significant decrease in the
200 expression of peroxisome proliferator-activated receptor (PPAR)-α, which regulates the
201 expression of genes involved in fatty acid oxidation, as well as that of PPAR-γ co-activator-
202 1α (PGC-1α) in the skeletal muscle of the denervated mice compared with that in the sham-
203 operated mice whereas there was no difference between D-ND and D-AR (Fig. 5). In contrast,
204 there was a significant difference in the expression of PPARδ and pyruvate dehydrogenase
205 kinase 4 (PDK4) in D-AR compared to that in D-ND (Fig. 5).
206
207 *3.4 Effect of dietary ARs on the expression of genes related to lipid droplets (LD)*
208 *formation and the abundance of LD-coated proteins in denervated mice.*

209 An analysis of the expression of genes related to LD formation revealed that there
210 was no difference among the four groups in the expression of phospholipase D1 (Pld1).
211 Although the mRNA transcription of the RAS oncogene family member Rab 18 in the
212 skeletal muscle of denervated mice was significantly higher than that in the sham-operated
213 mice, there was no difference between D-ND and D-AR (Fig. 6). The analysis of the
214 expression of genes related to the abundance of LD-coated proteins showed that the
215 expression of perilipin (Plin) 2 in the skeletal muscle of denervated mice was significantly
216 higher than that in the sham-operated mice. Moreover, the expression of Plin 2 was induced
217 to a higher level in D-AR than in D-ND (Fig. 6). In contrast, the expression of Plin 4 and 5 in
218 the skeletal muscle of denervated mice was significantly lower than that in the sham-operated
219 mice. The expression of Plin 4 and 5 in D-AR was slightly higher than that in D-ND (Fig. 6).
220

221 **4. Discussion**

222 In this study, we set the experiment 6 days after denervation which coincides to the early
223 stage of atrophy development. This may be possible that the accumulation of AR in muscle
224 could not be detected during this period. In our previous study, we reported that pre-intake of
225 flavonoid, quercetin for 14 days, suppressed reduction of muscle mass at 4 or 6 days after
226 denervation, whereas, 1-day pre-intake of quercetin did not prevent the reduction of muscle
227 mass [26]. Therefore, in the present study, we decided to continue ARs feeding for 34 days

including pre-intake for 28 days in order to account for effective prevention of muscle atrophy.

The results of this study demonstrated that the intake of ARs inhibited the decreases in the muscle mass and CSA of the myofibers in skeletal muscle that were caused by denervation. However, ARs failed to suppress the upregulation of the expression of muscle atrophy-associated ubiquitin ligases and autophagy. Additionally, there was no difference between D-ND and D-AR in the abundance of 4E-BP1 (data not shown), which is one of the protein synthesis-related proteins. It is possible that other factors contribute to the limitation of muscle mass loss by ARs. Interestingly, we found that the abundance of the autophagy marker p62 was significantly higher in D-AR than in D-ND (Fig. 4). Recently, it has been reported that p62 co-localized with LDs in L6 myocytes [27]. Moreover, p62 was found to interact with adipose differentiation-related protein, which is an LD membrane protein, implying that it regulates lipophagy to modulate the turnover of LDs. In addition, p62-deficient mice developed obesity, impaired glucose, and insulin intolerance [28]. These findings suggested that the intake of ARs may be associated with the degradation of lipids in atrophic muscle.

Activation of the autophagy-lysosome system has been demonstrated in a large number of atrophied muscles [29]. Among them, mitophagy specifically plays an important role in the selective degradation of impaired mitochondria in atrophied muscle [30, 31]. Previous report

has shown that muscle-specific knockout mice lacking autophagy-related (Atg) protein 7 developed severe muscle atrophy and age-dependent decrease in force, which implies that autophagy flux is essential for preservation of muscle mass and retention of myofiber integrity [32]. On the other hand, we found that ARs could possibly modify the disruption to fatty acid metabolism induced by lipid autophagy. Recently, it has been reported that lipophagy contributes to supplying energy from lipid and control lipid homeostasis [33]. These findings suggest the importance of mitophagy and lipophagy in the physiologic adaptation of muscle atrophy.

It has also been reported that the phenolic compound, epigallocatechin-3-gallate found in green tea induces lipophagy though the activation of adenosine monophosphate-activated protein kinase (AMPK) in vascular endothelial cells and adipocytes [34, 35]. Similarly, kaempferol, a natural flavonoid, improves accumulated lipid and increased ER stress through an AMPK/mTOR-mediated lipophagy pathway in pancreatic β-cells [36]. AMPK controls glucose and lipid metabolism in response to intracellular energy imbalance. Additionally, the activation of AMPK stimulates glucose transport by insulin independent signaling pathway [37]. Given that the fasting glucose level of ARs-fed mice was lower than that of the normal diet-fed mice, ARs may induce lipophagy through activation of AMPK. Further investigations are necessary to explore this mechanism.

265 Muscle atrophy caused by aging and inactivity is associated with the accumulation of
266 intramuscular triglycerides as well as a progressive loss of muscle mass [38]. It has been
267 reported that the regulation of the expression of perilipin, which is a known LD-associated
268 protein, contributes to sarcopenia and muscle weakness [39, 40]. These findings may reflect
269 the changed energy demand under the condition of muscle atrophy. Indeed, the expression of
270 Plin 2 was induced to a higher level in D-AR than in D-ND, while the expression of Plin 4
271 and 5 was slightly higher in D-AR than in D-ND (Fig. 6). Plin 2 and 4 were highly expressed
272 in type I (slow oxidative) fibers more than in type II (fast glycolytic) fibers [41, 42, 43].
273 Moreover, Plin 5 localizes with LDs and mitochondria in skeletal muscle, where it regulates
274 fatty acid oxidation [44]. Bosma et al. showed that the overexpression of Plin5 in skeletal
275 muscle promoted the expression of genes involved in fatty acid β-oxidation, tricarboxylic
276 acid cycle, electron transport chain, and, mitochondrion organization [45]. These findings
277 raise the possibility that the energy demand in the atrophied muscle of mice fed with the AR-
278 supplemented diet could be met by increased lipid oxidation.
279 PPARδ is an important transcription factor that is known as a regulator of muscle lipid
280 oxidation in skeletal muscle [46]. The expression of UCP3 and PDK4 is regulated by the
281 PPARδ pathway to modify fatty acid metabolism and regulate insulin sensitivity in skeletal
282 muscle [47, 48]. We found that the expression of PPARδ, UCP3, and PDK4 increased in the
283 atrophied muscle of the mice that were fed with ARs-supplemented diet (Fig. 5). PDK4 is a

key enzyme that downregulates glycolysis and upregulates lipid oxidation by inhibiting the synthesis of acetyl-CoA from pyruvate [48, 49]. Transgenic mice with the cardiac-specific overexpression of PDK4 showed enhanced fatty acid oxidation, but not glucose oxidation, preventing high fat diet-induced myocyte lipid accumulation [50]. In addition, transgenic mice with the skeletal muscle-specific overexpression of UCP3 showed an increased capacity for fatty acid uptake, fatty acid oxidation, and an increased whole-body fat oxidation [51]. These findings suggest that the main energy supply pathway in the atrophic muscle of mice fed with an ARs-supplemented diet shifted from glycolysis to fatty acid oxidation.

Acknowledgements

We are grateful to Dr. Yosuke Kikuch for helpful advice on the isolation of ARs from wheat bran. This research did not receive any specific grant from funding agencies in the public, commercial or non-for-profit sectors.

Conflict of interest

We declare that there is no conflict of interest.

301 **References**

302 [1] Rüegg MA, Glass DJ. Molecular mechanisms and treatment options for muscle
303 wasting diseases. Annu Rev Pharmacol Toxicol 2011;51:373-95.

304 [2] Bodine SC, Baehr LM. Skeletal muscle atrophy and the E3 ubiquitin ligases MuRF1
305 and MAFbx/atrogin-1. Am J Physiol Endocrinol Metab 2014;307:E469-84.

306 [3] Ogawa T, Furochi H, Mameoka M, Hirasaka K, Onishi Y, Suzue N, Oarada M,
307 Akamatsu M, Akima H, Fukunaga T, Kishi K, Yasui N, Ishidoh K, Fukuoka H,
308 Nikawa T. Ubiquitin ligase gene expression in healthy volunteers with 20-day
309 bedrest. Muscle Nerve 2006;34:463-9.

310 [4] Ikemoto M, Nikawa T, Takeda S, Watanabe C, Kitano T, Baldwin KM, Izumi R,
311 Nonaka I, Towatari T, Teshima S, Rokutan K, Kishi K. Space shuttle flight (STS-90)
312 enhances degradation of rat myosin heavy chain in association with activation of
313 ubiquitin-proteasome pathway. FASEB J 2001;15:1279-81.

314 [5] Bodine SC, Latres E, Baumhueter S, Lai VK, Nunez L, Clarke BA, Poueymirou WT,
315 Panaro FJ, Na E, Dharmarajan K, Pan ZQ, Valenzuela DM, DeChiara TM, Stitt TN,
316 Yancopoulos GD, Glass DJ. Identification of ubiquitin ligases required for skeletal
317 muscle atrophy. Science 2001;294:1704-8.

[6] Gomes MD, Lecker SH, Jagoe RT, Navon A, Goldberg AL. Atrogin-1, a muscle-specific F-box protein highly expressed during muscle atrophy. Proc Natl Acad Sci U S A 2001;98:14440-5.

[7] Zhao J, Brault JJ, Schild A, Cao P, Sandri M, Schiaffino S, Lecker SH, Goldberg AL. FoxO3 coordinately activates protein degradation by the autophagic/lysosomal and proteasomal pathways in atrophying muscle cells. Cell Metab 2007;6:472-83.

[8] Furuno K, Goodman MN, Goldberg AL. Role of different proteolytic systems in the degradation of muscle proteins during denervation atrophy. J Biol Chem 1990;265:8550-7.

[9] Argadine HM, Hellyer NJ, Mantilla CB, Zhan WZ, Sieck GC. The effect of denervation on protein synthesis and degradation in adult rat diaphragm muscle. J Appl Physiol 2009;107:438-44.

[10] Nwoye L, Mommaerts WF, Simpson DR, Seraydarian K, Marusich M. Evidence for a direct action of thyroid hormone in specifying muscle properties. Am J Physiol 1982;242:R401-8.

[11] Midrio M, Danieli-Betto D, Megighian A, Velussi C, Catani C, Carraro U. Slow-to-fast transformation of denervated soleus muscle of the rat, in the presence of an antifibrillatory drug. Pflugers Arch 1992;420:446-50.

[12] Nikawa T, Ishidoh K, Hirasaka K, Ishihara I, Ikemoto M, Kano M, Kominami E, Nonaka I, Ogawa T, Adams GR, Baldwin KM, Yasui N, Kishi K, Takeda S. Skeletal muscle gene expression in space-flown rats. FASEB J 2004;18:522-4.

[13] Lang F, Aravamudhan S, Nolte H, Türk C, Hölper S, Müller S, Günther S, Blaauw B, Braun T, Krüger M. Dynamic changes in the mouse skeletal muscle proteome during denervation-induced atrophy. Dis Model Mech 2017;10:881-896.

[14] Kris-Etherton PM, Hecker KD, Bonanome A, Coval SM, Binkoski AE, Hilpert KF, Griel AE, Etherton TD. Bioactive compounds in foods: their role in the prevention of cardiovascular disease and cancer. Am J Med 2002;113:71S-88S.

[15] Ye EQ, Chacko SA, Chou EL, Kugizaki M, Liu S. Greater whole-grain intake is associated with lower risk of type 2 diabetes, cardiovascular disease, and weight gain. J Nutr 2012;142:1304-13.

[16] He M, van Dam RM, Rimm E, Hu FB, Qi L. Whole-grain, cereal fiber, bran, and germ intake and the risks of all-cause and cardiovascular disease-specific mortality among women with type 2 diabetes mellitus. Circulation 2010;121:2162-8.

[17] McKeown NM, Jacques PF, Seal CJ, de Vries J, Jonnalagadda SS, Clemens R, Webb D, Murphy LA, van Klinken JW, Topping D, Murray R, Degeneffe D, Marquart LF. Whole grains and health: from theory to practice--highlights of The

Grains for Health Foundation's Whole Grains Summit 2012. J Nutr 2013;143:744S-758S.

[18] Ross AB, Kamal-Eldin A, Aman P. Dietary alkylresorcinols: absorption, bioactivities, and possible use as biomarkers of whole-grain wheat- and rye-rich foods. Nutr Rev 2004;62:81-95.

[19] Oishi K, Yamamoto S, Itoh N, Nakao R, Yasumoto Y, Tanaka K, Kikuchi Y, Fukudome S, Okita K, Takano-Ishikawa Y. Wheat alkylresorcinols suppress high-fat, high-sucrose diet-induced obesity and glucose intolerance by increasing insulin sensitivity and cholesterol excretion in male mice. J Nutr 2015;145:199-206.

[20] Fujiwara Y, Tsukahara C, Ikeda N, Sone Y, Ishikawa T, Ichi I, Koike T, Aoki Y. Oleuropein improves insulin resistance in skeletal muscle by promoting the translocation of GLUT4. J Clin Biochem Nutr 2017:61:196-202.

[21] Szychlinska MA, Castrogiovanni P, Trovato FM, Nsir H, Zarrouk M, Lo Furno D, Di Rosa M, Imbesi R, Musumeci G. Physical activity and Mediterranean diet based on olive tree phenolic compounds from two different geographical areas have protective effects on early osteoarthritis, muscle atrophy and hepatic steatosis. Eur J Nutr 2018:doi: 10.1007/s00394-018-1632-2.

[22] Hirasaka K, Saito S, Yamaguchi S, Miyazaki R, Wang Y, Haruna M, Taniyama S, Higashitani A, Terao J, Nikawa T, Tachibana K. Dietary Supplementation with

Isoflavones Prevents Muscle Wasting in Tumor-Bearing Mice. J Nutr Sci Vitaminol (Tokyo) 2016;62:178-84.

[23] Dianita R, Jantan I, Amran AZ, Jalil J. Protective effects of Labisia pumila var. alata on biochemical and histopathological alterations of cardiac muscle cells in isoproterenol-induced myocardial infarction rats. Molecules 2015;20:4746-63.

[24] Mammucari C, Milan G, Romanello V, Masiero E, Rudolf R, Del Piccolo P, Burden SJ, Di Lisi R, Sandri C, Zhao J, Goldberg AL, Schiaffino S, Sandri M. FoxO3 controls autophagy in skeletal muscle in vivo. Cell Metab 2007;6:458-71.

[25] Singh R, Kaushik S, Wang Y, Xiang Y, Novak I, Komatsu M, Tanaka K, Cuervo AM, Czaja MJ. Autophagy regulates lipid metabolism. Nature 2009;458:1131-5.

[26] Mukai R, Matsui N, Fujikura Y, Matsumoto N, Hou DX, Kanzaki N, Shibata H, Horikawa M, Iwasa K, Hirasaka K, Nikawa T, Terao J. Preventive effect of dietary quercetin on disuse muscle atrophy by targeting mitochondria in denervated mice. J Nutr Biochem 2016;31:67-76.

[27] Lam T, Harmancey R, Vasquez H, Gilbert B, Patel N, Hariharan V, Lee A, Covey M, Taegtmeyer H. Reversal of intramyocellular lipid accumulation by lipophagy and a p62-mediated pathway. Cell Death Discov 2016;2:16061.

391 [28] Rodriguez A, Durán A, Selloum M, Champy MF, Diez-Guerra FJ, Flores JM,
392 Serrano M, Auwerx J, Diaz-Meco MT, Moscat J. Mature-onset obesity and insulin
393 resistance in mice deficient in the signaling adapter p62. Cell Metab 2006;3:211-22.
394 [29] Bechet D, Tassa A, Taillandier D, Combaret L, Attaix D. Lysosomal proteolysis in
395 skeletal muscle. Int J Biochem Cell Biol 2005:37:2098-114.
396 [30] Mammucari C, Milan G, Romanello V, Masiero E, Rudolf R, Del Piccolo P, Burden
397 SJ, Di Lisi R, Sandri C, Zhao J, Goldberg AL, Schiaffino S, Sandri M. FoxO3
398 controls autophagy in skeletal muscle in vivo. Cell Metab 2007:6:458-71.
399 [31] Kang C, Ji LL. PGC-1α overexpression via local transfection attenuates mitophagy
400 pathway in muscle disuse atrophy. Free Radic Biol Med 2016:93:32-40.
401 [32] Masiero E, Agatea L, Mammucari C, Blaauw B, Loro E, Komatsu M, Metzger D,
402 Reggiani C, Schiaffino S, Sandri M. Autophagy is required to maintain muscle mass.
403 Cell Metab 2009:10:507-15.
404 [33] Garcia EJ, Vevea JD, Pon LA. Lipid droplet autophagy during energy mobilization,
405 lipid homeostasis and protein quality control. Front Biosci 2018:23:1552-63.
406 [34] Kim HS, Montana V, Jang HJ, Parpura V, Kim JA. Epigallocatechin gallate (EGCG)
407 stimulates autophagy in vascular endothelial cells: a potential role for reducing lipid
408 accumulation. J Biol Chem 2013:288:22693-705.

[35] Kim SN, Kwon HJ, Akindehin S, Jeong HW, Lee YH. Effects of Epigallocatechin-3-Gallate on Autophagic Lipolysis in Adipocytes. Nutrients 2017:9:E680.

[36] Varshney R, Varshney R, Mishra R, Gupta S, Sircar D, Roy P. Kaempferol alleviates palmitic acid-induced lipid stores, endoplasmic reticulum stress and pancreatic β-cell dysfunction through AMPK/mTOR-mediated lipophagy. J Nutr Biochem 2018:57:212-27.

[37] Hayashi T, Hirshman MF, Kurth EJ, Winder WW, Goodyear LJ. Evidence for 5' AMP-activated protein kinase mediation of the effect of muscle contraction on glucose transport. Diabetes 1998:47:1369-73.

[38] Marcus RL, Addison O, Kidde JP, Dibble LE, Lastayo PC. Skeletal muscle fat infiltration: impact of age, inactivity, and exercise. J Nutr Health Aging 2010;14:362-6.

[39] Conte M, Vasuri F, Bertaggia E, Armani A, Santoro A, Bellavista E, Degiovanni A, D'Errico-Grigioni A, Trisolino G, Capri M, Franchi MV, Narici MV, Sandri M, Franceschi C, Salvioli S. Differential expression of perilipin 2 and 5 in human skeletal muscle during aging and their association with atrophy-related genes. Biogerontology 2015;16:329-40.

[40] Conte M, Vasuri F, Trisolino G, Bellavista E, Santoro A, Degiovanni A, Martucci E, D'Errico-Grigioni A, Caporossi D, Capri M, Maier AB, Seynnes O, Barberi L,

Musarò A, Narici MV, Franceschi C, Salvioli S. Increased Plin2 expression in human skeletal muscle is associated with sarcopenia and muscle weakness. PLoS One 2013;8:e73709.

[41] Shaw CS, Shepherd SO, Wagenmakers AJ, Hansen D, Dendale P, van Loon LJ. Prolonged exercise training increases intramuscular lipid content and perilipin 2 expression in type I muscle fibers of patients with type 2 diabetes. Am J Physiol Endocrinol Metab 2012;303:E1158-65.

[42] Shaw CS, Sherlock M, Stewart PM, Wagenmakers AJ. Adipophilin distribution and colocalization with lipid droplets in skeletal muscle. Histochem Cell Biol 2009;131:575-81.

[43] Pourteymour S, Lee S, Langleite TM, Eckardt K, Hjorth M, Bindesbøll C, Dalen KT, Birkeland KI, Drevon CA, Holen T, Norheim F. Perilipin 4 in human skeletal muscle: localization and effect of physical activity. Physiol Rep 2015;3:e12481.

[44] Bosma M, Minnaard R, Sparks LM, Schaart G, Losen M, de Baets MH, Duimel H, Kersten S, Bickel PE, Schrauwen P, Hesselink MK. The lipid droplet coat protein perilipin 5 also localizes to muscle mitochondria. Histochem Cell Biol 2012;137:205-16.

[45] Bosma M, Sparks LM, Hooiveld GJ, Jorgensen JA, Houten SM, Schrauwen P, Kersten S, Hesselink MK. Overexpression of PLIN5 in skeletal muscle promotes

oxidative gene expression and intramyocellular lipid content without compromising insulin sensitivity. Biochim Biophys Acta 2013;1831:844-52.

[46] Ehrenborg E, Krook A. Regulation of skeletal muscle physiology and metabolism by peroxisome proliferator-activated receptor delta. Pharmacol Rev 2009;61:373-93.

[47] MacLellan JD, Gerrits MF, Gowing A, Smith PJ, Wheeler MB, Harper ME. Physiological increases in uncoupling protein 3 augment fatty acid oxidation and decrease reactive oxygen species production without uncoupling respiration in muscle cells. Diabetes 2005;54:2343-50.

[48] Sugden MC, Holness MJ. Recent advances in mechanisms regulating glucose oxidation at the level of the pyruvate dehydrogenase complex by PDKs. Am J Physiol Endocrinol Metab 2003;284:E855-62.

[49] Wu P, Sato J, Zhao Y, Jaskiewicz J, Popov KM, Harris RA. Starvation and diabetes increase the amount of pyruvate dehydrogenase kinase isoenzyme 4 in rat heart. Biochem J 1998;329:197-201.

[50] Chambers KT, Leone TC, Sambandam N, Kovacs A, Wagg CS, Lopaschuk GD, Finck BN, Kelly DP. Chronic inhibition of pyruvate dehydrogenase in heart triggers an adaptive metabolic response. J Biol Chem 2011;286:11155-62.

[51] Bezaire V, Spriet LL, Campbell S, Sabet N, Gerrits M, Bonen A, Harper ME. Constitutive UCP3 overexpression at physiological levels increases mouse skeletal muscle capacity for fatty acid transport and oxidation. FASEB J 2005;19:977-9.

472 **Table 1.** Changes in body weight and food intake of denervated mice fed a normal or ARs

473 diet.

Groups	S-ND	D-ND	S-AR	D-AR
n	5	6	5	6
Body weight (g)	28.0 ± 0.6^{ab}	29.7 ± 0.7^{a}	26.8 ± 0.4^{bc}	25.4 ± 0.5^{c}
Food intake (g)	3.8 ± 0.6^{a}	3.1 ± 0.4^{a}	3.4 ± 0.2^{a}	3.8 ± 0.5^{a}

474 Data are mean ± SEM (n = 5–6). Different letters indicate significant differences ($P < 0.05$)

475 based on ANOVA and Tukey-Kramer test. S-ND, sham-operated (control) mice fed with

476 normal diet; D-ND, denervated mice fed with normal diet; S-AR, control mice fed with ARs-

477 supplemented diet; D-AR, denervated mice fed the ARs-supplemented diet.

478

Figure legends

Fig. 1. The effect of dietary alkylresorcinols (ARs) on the denervation-induced decrease in the wet weight of skeletal muscle. An ARs-supplemented diet or a normal diet was given to mice for 4 weeks, and then their skeletal muscles were isolated 6 days after denervation. The wet weights of the tibialis anterior (TA), extensor digitorum longus (EDL), gastrocnemius (GA), and soleus (SO) muscles were measured. Data are mean ± SEM (n = 5–6). Different letters indicate significant differences ($P < 0.05$) based on ANOVA and Tukey-Kramer test. S-ND, sham-operated (control) mice fed the normal diet; D-ND, denervated mice fed the normal diet; S-AR, control mice fed the ARs-supplemented diet; D-AR, denervated mice fed the ARs-supplemented diet.

Fig. 2. Effect of dietary ARs on the denervation-induced decrease in muscle cross-sectional area (CSA). (A) Representative sections (5-μm thickness) from the GA muscle of denervated mice on day 6 were stained with hematoxylin and eosin. Scale bar = 100 μm. (B) The distributions of CSAs indicate the ratio of the number of myofibers with the indicated area to the total number of myofibers in the section. S-ND, sham-operated (control) mice fed the normal diet; D-ND, denervated mice fed the normal diet; S-AR, control mice fed the ARs-supplemented diet; D-AR, denervated mice fed the ARs-supplemented diet.

497 Fig. 3. Effect of dietary ARs on the expression of ubiquitin ligase- and autophagy-related
498 genes in the denervated muscle of mice. The total RNA of gastrocnemius muscle was
499 extracted and subjected to real-time reverse transcription-polymerase chain reaction. The
500 ratio between the intensities of ubiquitin ligase- or autophagy-related genes and 18S
501 ribosomal RNA was calculated. Data are mean ± SEM (n = 5-6). Different letters indicate
502 significant differences ($P < 0.05$) based on ANOVA and Tukey-Kramer test. S-ND, sham-
503 operated (control) mice fed the normal diet; D-ND, denervated mice fed the normal diet; S-
504 AR, control mice fed the ARs-supplemented diet; D-AR, denervated mice fed the ARs-
505 supplemented diet.

506

507 Fig. 4. Effect of ARs on the activation of autophagy and protein synthesis in the denervated
508 muscle of mice. Proteins (20 μg/lane) extracted from the GA muscle were subjected to
509 sodium dodecyl sulfate-polyacrylamide gel electrophoresis and transferred to a
510 polyvinylidene difluoride membrane. Immunoblotting for LC3b, p62, and GAPDH was
511 performed on different membranes without antibody stripping, as described in the Materials
512 and Methods. The ratio of p62 and LC3-II protein to GAPDH was calculated by
513 densitometric analysis. Data are mean ± SEM (n = 5-6). Different letters indicate significant
514 differences ($P < 0.05$) based on ANOVA and Tukey-Kramer test. S-ND, sham-operated

515 (control) mice fed the normal diet; D-ND, denervated mice fed the normal diet; S-AR, control
516 mice fed the ARs-supplemented diet; D-AR, denervated mice fed the ARs-supplemented diet.

517 Fig. 5. Effect of dietary ARs on the expression of energy metabolism-related genes in the
518 denervated muscle of mice. The total RNA of gastrocnemius muscle was extracted and
519 subjected to real-time reverse transcription-polymerase chain reaction. The ratio between the
520 intensities of energy metabolism-related genes and 18S ribosomal RNA was calculated. Data
521 are mean ± SEM (n = 5-6). Different letters indicate significant differences ($P < 0.05$) based
522 on ANOVA and Tukey-Kramer test. S-ND, sham-operated (control) mice fed the normal
523 diet; D-ND, denervated mice fed the normal diet; S-AR, control mice fed the ARs-
524 supplemented diet; D-AR, denervated mice fed the ARs-supplemented diet.

525

526 Fig. 6. Effect of dietary ARs on lipid droplets (LD) formation and the expression of LD-
527 coated proteins-related genes in the denervated muscle of mice. Total RNA of gastrocnemius
528 muscle was extracted and subjected to real-time RT-PCR. The ratio of the intensities of genes
529 related to LD formation and the abundance of LD-coated proteins to that of 18S ribosomal
530 RNA was calculated. Data are mean ± SEM (n = 5-6). Different letters indicate significant
531 differences ($P < 0.05$) based on ANOVA and Tukey-Kramer test. S-ND, sham-operated
532 (control) mice fed the normal diet; D-ND, denervated mice fed the normal diet; S-AR, control
533 mice fed the ARs-supplemented diet; D-AR, denervated mice fed the ARs-supplemented diet.

Fig. 1

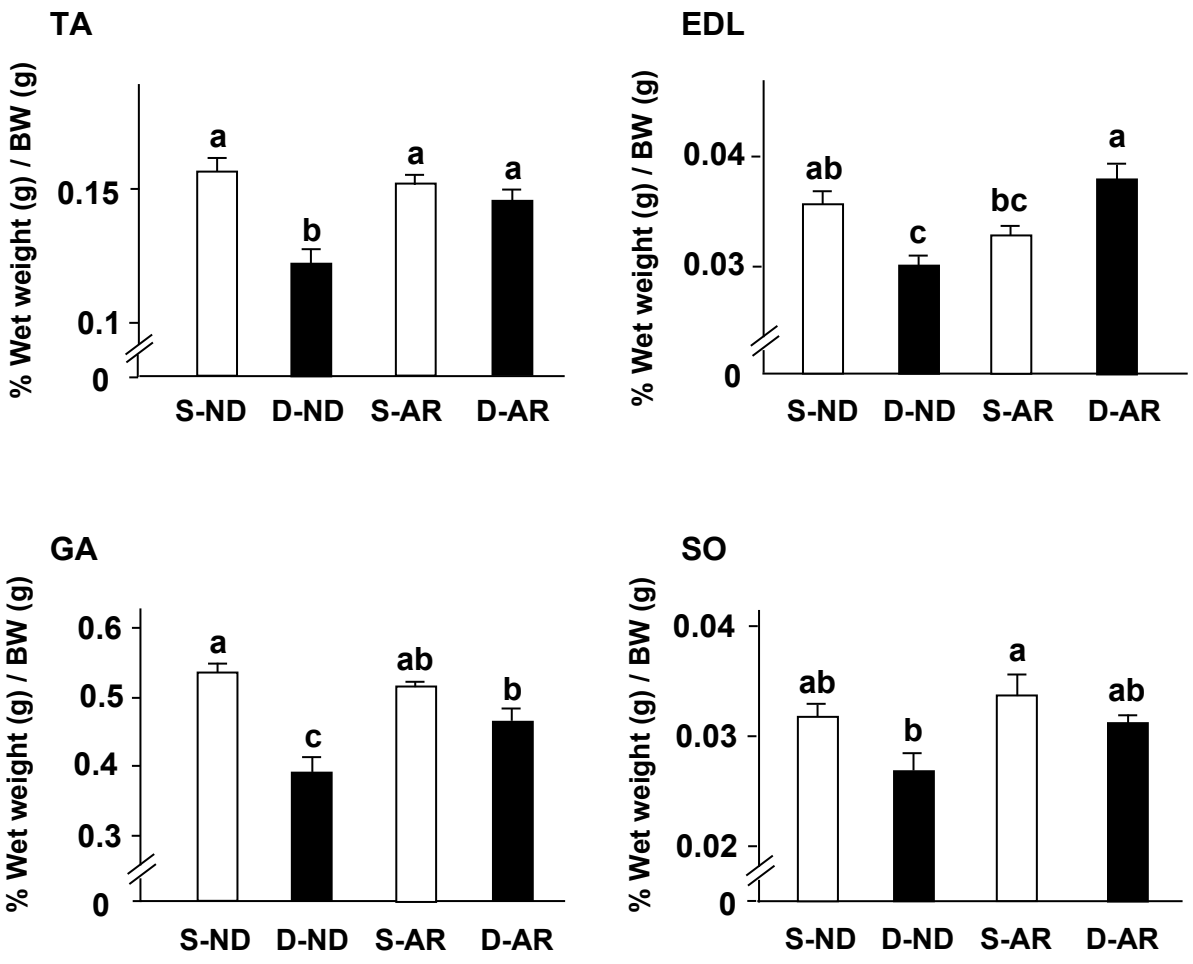
TA
% Wet weight (g) / BW (g)
0.15
0.1
0
a
b
a
a
S-ND
D-ND
S-AR
D-AR
EDL
% Wet weight (g) / BW (g)
0.04
0.03
0
ab
c
bc
a
S-ND
D-ND
S-AR
D-AR
GA
% Wet weight (g) / BW (g)
0.6
0.5
0.4
0.3
0
a
c
ab
b
S-ND
D-ND
S-AR
D-AR
SO
% Wet weight (g) / BW (g)
0.04
0.03
0.02
0
ab
b
a
ab
S-ND
D-ND
S-AR
D-AR

Fig. 2

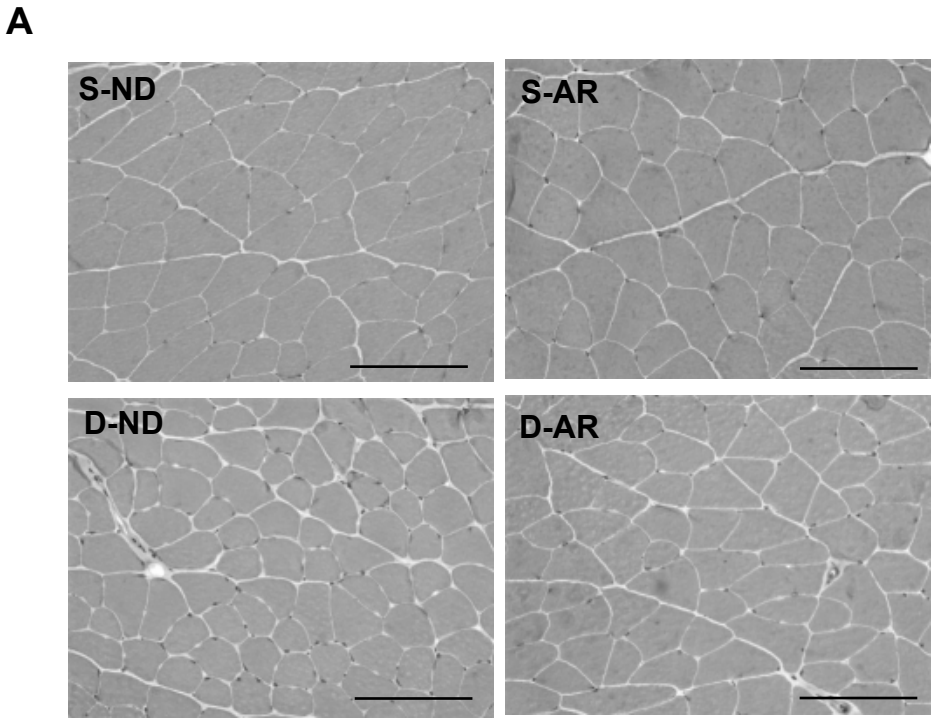
A
S-ND
S-AR
D-ND
D-AR
B
S-ND
S-AR
D-ND
D-AR
% myofiber
60
40
20
0
0 - 500
501 - 1000
1001 - 1500
1501 - 2000
2001 - 2500
2501 -
(μm²)

Fig. 3

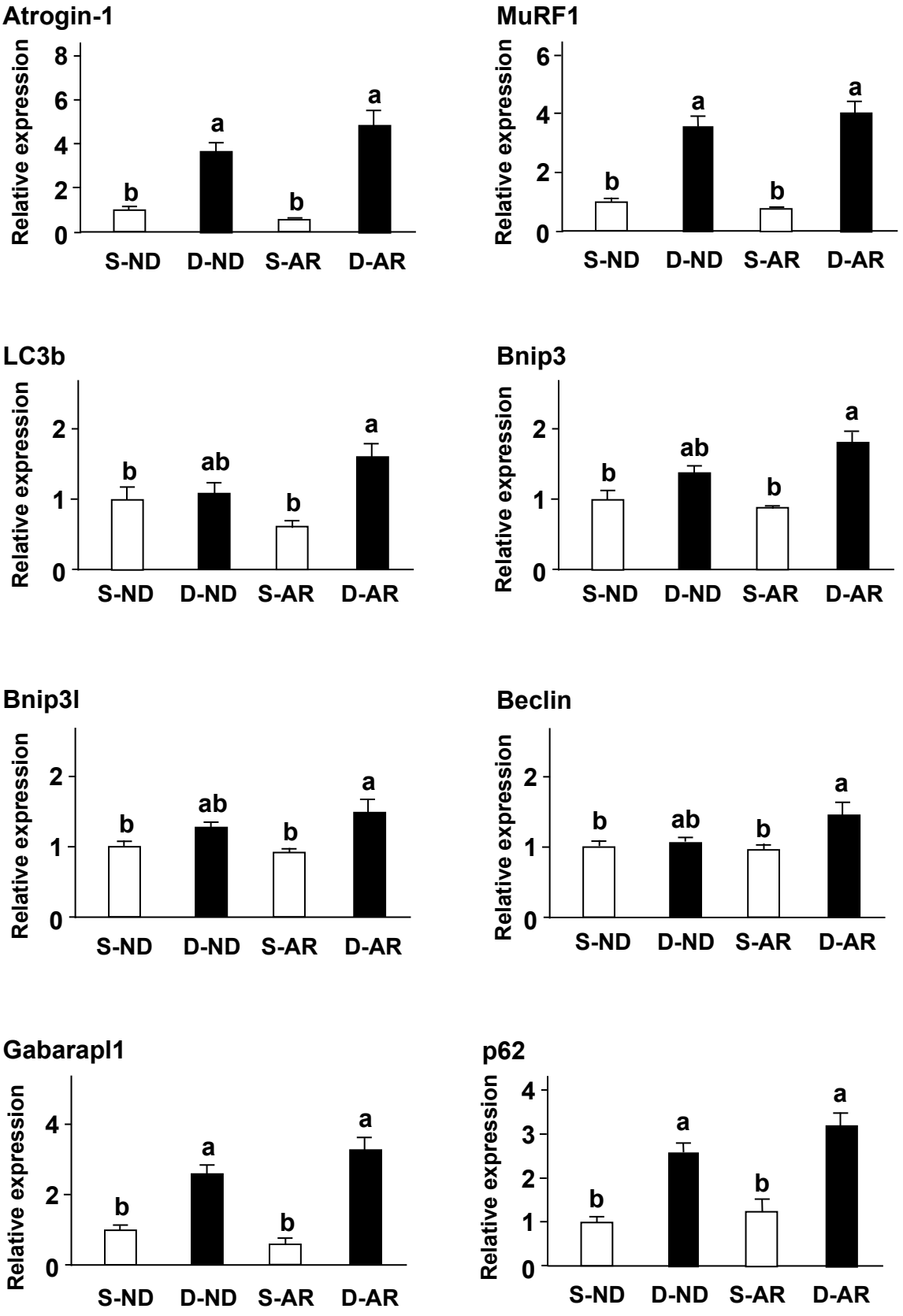
Atrogin-1
Relative expression
8
6
4
2
0
b
a
b
a
S-ND
D-ND
S-AR
D-AR
MuRF1
Relative expression
6
4
2
0
b
a
b
a
S-ND
D-ND
S-AR
D-AR
LC3b
Relative expression
2
1
0
b
ab
b
a
S-ND
D-ND
S-AR
D-AR
Bnip3
Relative expression
2
1
0
b
ab
b
a
S-ND
D-ND
S-AR
D-AR
Bnip3l
Relative expression
2
1
0
b
ab
b
a
S-ND
D-ND
S-AR
D-AR
Beclin
Relative expression
2
1
0
b
ab
b
a
S-ND
D-ND
S-AR
D-AR
Gabarapl1
Relative expression
4
2
0
b
a
b
a
S-ND
D-ND
S-AR
D-AR
p62
Relative expression
4
3
2
1
0
b
a
b
a
S-ND
D-ND
S-AR
D-AR

Fig. 4

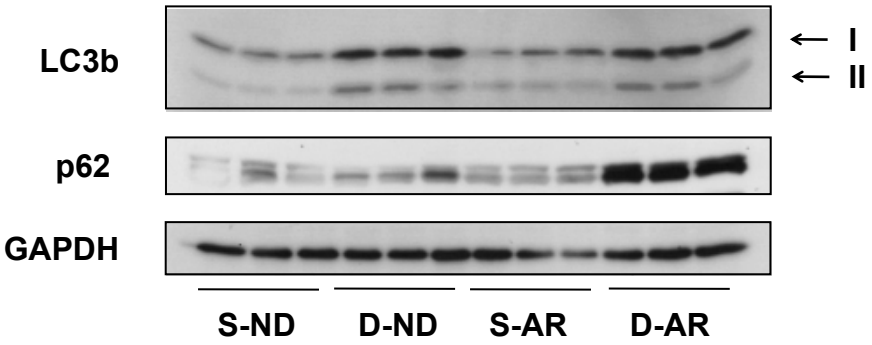
LC3b
p62
GAPDH
I
II
S-ND
D-ND
S-AR
D-AR

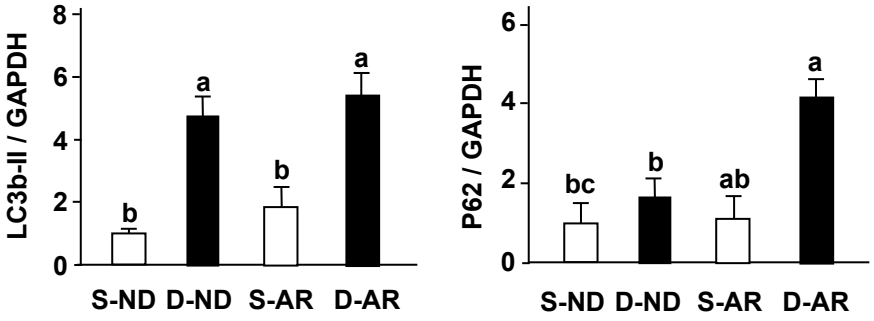
LC3b-II / GAPDH
8
6
4
2
0
b
a
b
a
S-ND D-ND S-AR D-AR
P62 / GAPDH
6
4
2
0
bc
b
ab
a
S-ND D-ND S-AR D-AR

Fig. 5

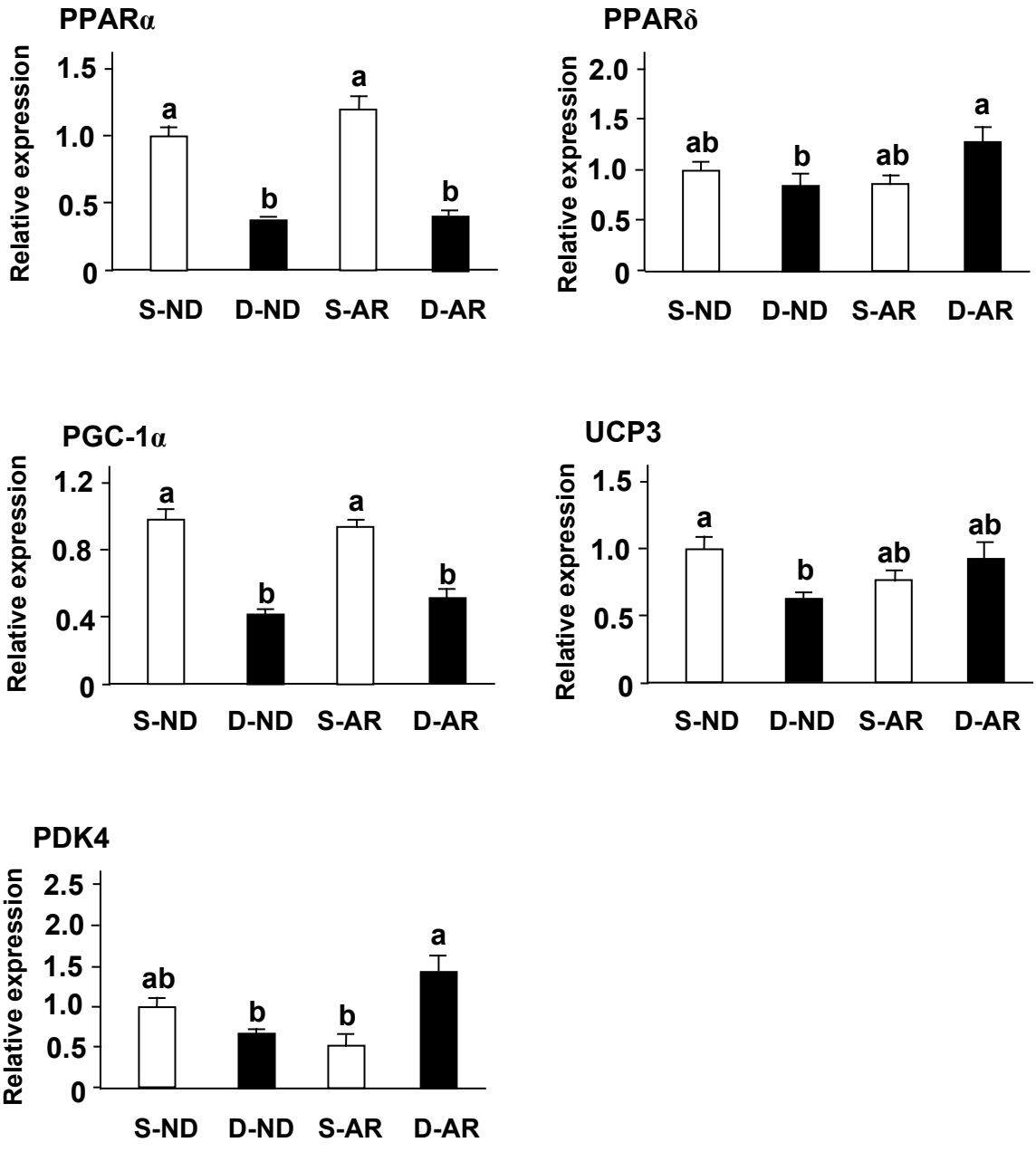
PPARα
Relative expression
1.5
1.0
0.5
0
a
b
a
b
S-ND
D-ND
S-AR
D-AR
PPARδ
Relative expression
2.0
1.5
1.0
0.5
0
ab
b
ab
a
S-ND
D-ND
S-AR
D-AR
PGC-1α
Relative expression
1.2
0.8
0.4
0
a
b
a
b
S-ND
D-ND
S-AR
D-AR
UCP3
Relative expression
1.5
1.0
0.5
0
a
b
ab
ab
S-ND
D-ND
S-AR
D-AR
PDK4
Relative expression
2.5
2.0
1.5
1.0
0.5
0
ab
b
b
a
S-ND
D-ND
S-AR
D-AR

Fig. 6

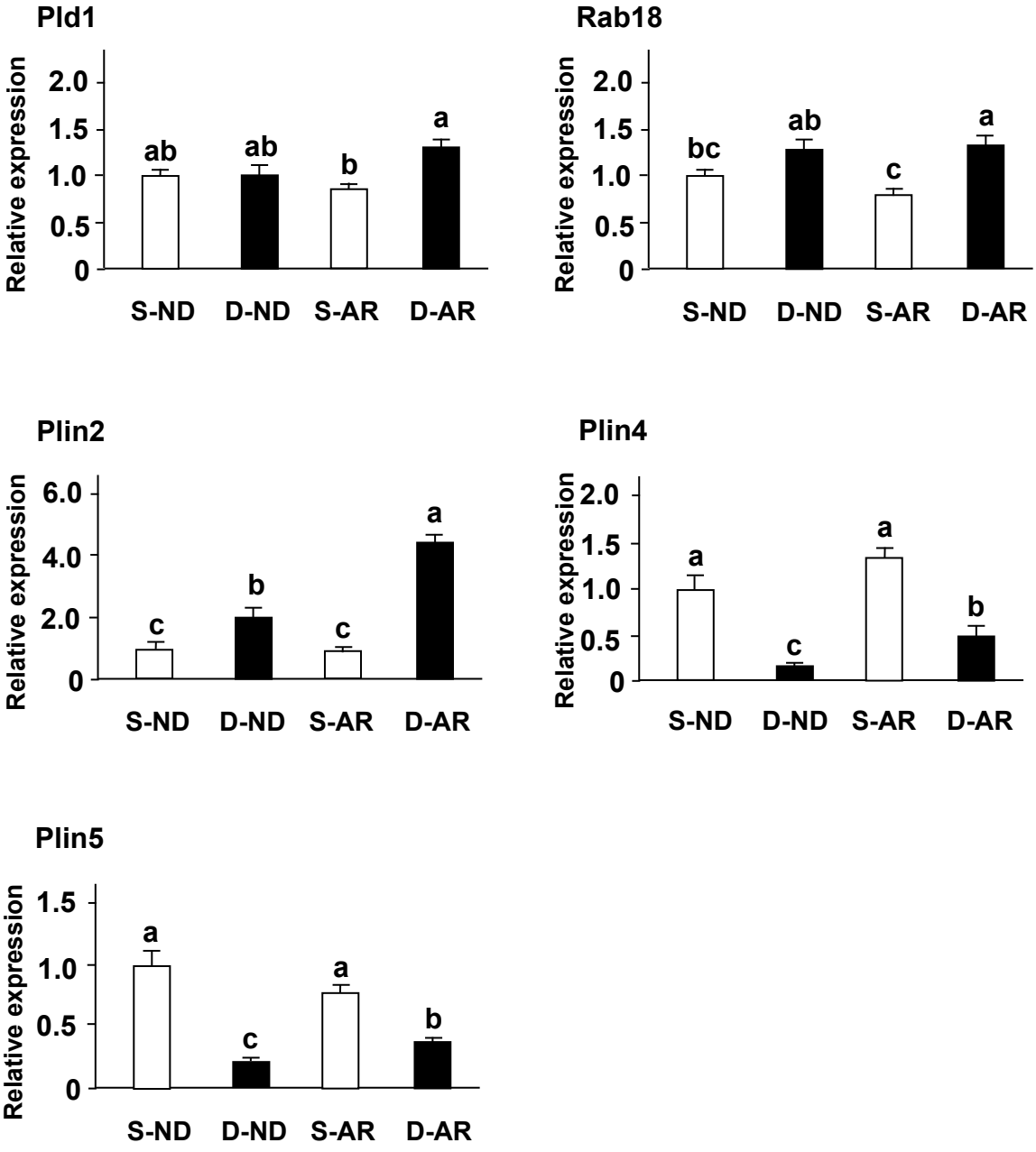
Pld1
Relative expression
2.0
1.5
1.0
0.5
0
ab
ab
b
a
S-ND
D-ND
S-AR
D-AR
Rab18
Relative expression
2.0
1.5
1.0
0.5
0
bc
ab
c
a
S-ND
D-ND
S-AR
D-AR
Plin2
Relative expression
6.0
4.0
2.0
0
c
b
c
a
S-ND
D-ND
S-AR
D-AR
Plin4
Relative expression
2.0
1.5
1.0
0.5
0
a
c
a
b
S-ND
D-ND
S-AR
D-AR
Plin5
Relative expression
1.5
1.0
0.5
0
a
c
a
b
S-ND
D-ND
S-AR
D-AR

Supplementary Table 1 Primer sets used in this study

Target gene		Sequence
Atrogin-1	S	5’- GGCGGACGGCTGGAA -3’
	AS	5’- CAGATTCTCCTTACTGTATACCTCCTTGT -3’
MuRF1	S	5’- TGCCTGGAGATGTTTACCAAGC -3’
	AS	5’- AAACGACCTCCAGACATGGACA -3’
MAP1-LC3b	S	5’- CACTGCTCTGTCTTGTGTAGGTTG -3’
	AS	5’- TCGTTGTGCCTTTATTAGTGCATC -3’
Gabarapl1	S	5’- CATCGTGGAGAAGGCTCCTA -3’
	AS	5’- ATACAGCTGGCCCATGGTAG -3’
Bnip3	S	5’- TTCCACTAGCACCTTCTGATGA -3’
	AS	5’- GAACACCGCATTTACAGAACAA -3’
Bnip3l	S	5’- TTGGGGCATTTTACTAACCTTG -3’
	AS	5’- TGCAGGTGACTGGTGGTACTAA -3’
Beclin	S	5’- TGAATGAGGATGACAGTGAGCA -3’
	AS	5’- CACCTGGTTCTCCACACTCTTG -3’

p62	S	5’- CTTCGGAAGCTGAAACATGG -3’
	AS	5’- GACTCAGCTGTAGGGCAAGG -3’
UCP3	S	5’- GGAGTCTCACCTGTTTACTGACAACT -3’
	AS	5’- GCACAGAAGCCAGCTCCAA -3’
PDK4	S	5’- AAAGGACAGGATGGAAGGAATCA -3’
	AS	5’- TTTTCCTCTGGGTTTGCACAT -3’
PGC-1α	S	5’- GAGGAAAGGAAGACTAAACGGCCA -3’
	AS	5’- GCCAGTCACAGGAGGCATCTTT -3’
PPARα	S	5’- CCTCAGGGTACCACTACGGAGT-3’
	AS	5’- GCCGAATAGTTCGCCGAA-3’
PPARδ	S	5’- GAGGGGTGCAAGGGCTTCTT-3’
	AS	5’- CACTTGTTGCGGTTCTTCTTCTG-3’
Pld1	S	5’- ATCGGTGATGGATGGAAAGG -3’
	AS	5’- CCCAGGACAAGTCTGAAGCA -3’
Rab18	S	5’- AGGACGTGCTGACCACTCTG -3’
	AS	5’- TGTGAACCTCAGGAGCAGGC -3’
Plin2	S	5’- GGGTGGAGTGGAAGAGAAGC -3’

	AS	5’- GAGCTGCTGGGTCAGGTTG -3’
	S	5’- GCTGCATGTGGGAAGCTGT -3’
Plin4		
	AS	5’- GTGCACAGCCTGTCCTGAG -3’
	S	5’- CCAGTTGGCCACAGTGAATG -3’
Plin5		
	AS	5’- GGCTGATGTCACCACCATGT -3’
	S	5’- GTAACCCGTTGAACCCCATT -3’
18S		
	AS	5’- CCATCCAATCGGTAGTAGCG - 3’

AS, antisense primer; S, sense primer; UCP, uncoupling protein; PDK, pyruvate dehydrogenase kinase; PPAR, peroxisome proliferator-activated receptor; PGC-1α, PPAR gamma coactivator 1 alpha; GAPDH, glycelaldehyde-3-phosphate dehydrogenase; MAP1-LC3b, microtubule-associated protein 1 light chain 3 beta; Gabarapl1, gamma-aminobutyric acid (GABA) A receptor-associated protein-like 1; Bnip3, BCL2/adenovirus E1B interacting protein 3; Bnip3l, BCL2/adenovirus E1B interacting protein 3-like; Pld1, phospholipase D1; Rab18, RAS oncogene family member Rab 18; Plin, perilipin,; 18S, 18S ribosomal RNA.